REDUCED CALIBRATION BY EFFICIENT TRANSFORMATION OF TEMPLATES FOR HIGH SPEED HYBRID CODED SSVEP BRAIN–COMPUTER INTERFACES

Kaori Suefusa and Toshihisa Tanaka

Department of Electronic and Information Engineering,
Tokyo University of Agriculture and Technology
Nakacho, Koganei-shi, Tokyo, 184–8588, Japan
Email: suefusa@sip.tuat.ac.jp, tanakat@cc.tuat.ac.jp

ABSTRACT

Brain–computer interfacing (BCI) based on steady-state visual evoked potentials (SSVEPs) is one of the most promising techniques due to its high performance. A state-of-the-art is a BCI based on hybrid frequency and phase coded SSVEP, which needs a large set of calibration data as reference signals, so-called individual templates. The aim of this study is to propose an approach to calibration reduction by generating from individual templates corresponding to a part of commands (*source templates*) to new templates corresponding to the rest of commands. The new templates can be obtained by shifting the frequency and phase of the source template to the desired frequency and phase. In this way, time and cost for calibration can be greatly reduced. The experimental results suggested that the proposed approach successfully transferred the source template, closely achieving the performance using the full calibration dataset.

Index Terms— Brain–computer interfacing, Steady-state visual evoked potentials, Hybrid frequency and phase coding.

1. INTRODUCTION

Brain–computer interfacing (BCI) has emerged as a potential application of signal processing, machine learning, and neuroscience. It provides a communication pathway between a brain and an external world, which enables people with severe motor disabilities to communicate and control devices without muscular movements [1, 2]. Over the decades, diverse BCIs based on features which can be observed in electroencephalography (EEG) have been proposed [1–10]. Specifically, steady-state visual evoked potentials (SSVEPs), which are cortical responses to a periodic visual stimulus, enable BCIs to achieve superior performance compared to the other EEG features [11].

Since SSVEPs are phase-locked periodic with the same or integer multiples of the frequency of visual stimulus, multiple commands can be implemented on SSVEP-BCIs by assigning different frequencies and/or phases to each stimulus. The method which assigns both frequencies and phases is called hybrid frequency and phase coding [12]. In terms of hybrid frequency and phase coding, there are two types of strategies: *mixed frequency and phase coding* and *joint frequency and phase coding*. Mixed coding implements $N_f \times N_p$ visual stimuli in total by assigning N_f different frequencies with each phase and N_p different phases with each frequency to a visual stimulus [13]. Besides, joint coding implements N_f visual stimuli in total by assigning N_f different frequencies to each visual stimulus and assigning different phases to two adjacent stimuli [12, 14]. Both strategies have been gaining attention [11, 15, 16], and it has been reported that both can achieve a high performance with a large number of commands [12].

Simultaneously with increasing the number of visual stimuli presented by the hybrid frequency and phase coding, algorithms for recognizing the frequency and phase of SSVEPs have also been improved [11, 15, 16]. A previous study on a mixed-coded SSVEP-BCI [15] proposed a method utilizing a calibration data, which significantly outperformed other canonical correlation analysis (CCA)-based methods. In the method, an average of EEG signals in a calibration dataset across trials, so-called an individual template or a training reference signal, is used as a reference signal which efficiently characterizes temporal features of each individual's SSVEPs. Recently, further improved algorithms based on the individual templates have been reported [11, 16]. A major issue which still remains on these algorithms is that they require a long time for calibration to obtain an acceptable individual template. The minimum time for calibration can be estimated as *a few seconds for one trial* $\times$ *the number of trials for each command* $\times$ *the number of commands*. For instance, with the settings in [11], the minimum time for calibration is 8 minutes (1 second for a trial $\times$ 12 trials for each command $\times$ 40 commands in total) for calibration without any rest in between sessions. Such a calibration step can take a lot of time and energy and might cause a visual fatigue before an actual use. To deal with the problem, Yuan *et al.* proposed an approach for joint-coded SSVEP-BCIs exploiting inter-subject information [17]. The method exploits the existing calibration data which were recorded beforehand by multiple users and averages their EEG signals to obtain templates for a new user, which enabled the new user to achieve a sufficient accuracy without any calibration. Although the method does not require any calibration for a new user, it is still necessary to have an access to an enormous calibration dataset of multiple users recorded in the same situation including electrode positions, visual stimuli, and so on.

To overcome this issue, we utterly propose a novel approach to calibration reduction by transferring the individual template of a certain command, called a *source template*, to obtain new templates of the other commands, called *target templates*. The target templates are generated by shifting the frequency and phase of the source template to the desired frequency and phase. An experiment with a mixed-coded SSVEP-BCI was conducted to evaluate performance of the proposed method in terms of the recognition accuracy.

This work is supported in part by JSPS Research Fellowship 16J08755 and JSPS KAKENHI Grant Number 15H04002. Toshihisa Tanaka is also affiliated with RIKEN Brain Science Institute, Saitama, Japan.

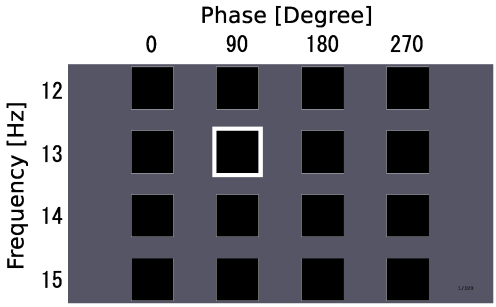

Fig. 1: Image of presented visual stimuli that reversed black/white pattern. Subjects were instructed to gaze at a stimulus framed by a white rectangle.

2. MATERIALS AND METHODS

2.1. Data Acquisition

Ten males and one female in their twenties took part in our experiment. All subjects were healthy and had normal or corrected-to-normal vision. They were given an informed consent, and this study was approved by the research ethics committee of Tokyo University of Agriculture and Technology.

A 23 inch LCD screen (BenQ, XL2411T) with a refresh rate of 120 Hz was used for displaying visual stimuli. During the experiment, the subjects seated on a comfortable chair in front of the screen about 60 cm away. Fig. 1 shows an image of displayed visual stimuli. As depicted in Fig. 1, sixteen visual stimuli corresponding to each command were displayed on the screen. All stimuli were approximately 5 centimeters on a side and disposed at equal intervals. Visual stimuli on each row flickered with frequencies of 12, 13, 14, or 15 Hz, respectively, and those on each column flickered with phases of 0, 90, 180, or 270 degrees, respectively. To present such flickering stimuli, an approximation approach *et al.* [18] was employed.

The subjects performed the following task in one trial. They started a trial by pressing the Enter key. One trial was configured with 1.5 seconds of pre-flickering interval, 4.0 seconds of flickering time, and 1.5 seconds of post-flickering interval. In pre-flickering interval, non-flickering visual stimuli and a white rectangle were displayed. In flickering time, all stimuli started flickering and the subjects were asked to gaze at the instructed stimulus by the white rectangle. In post-flickering interval all stimuli stopped flickering. After each trial, the task was stopped and the subjects were asked to rest their eyes. The task was restarted when the subjects pressed the Enter key again. 20 trials were performed with respect to each stimulus in a random order. Thus, each subject performed 320 trials in total.

To record EEG signals, we used Ag/AgCl active electrodes of Guger Technologies (g.tec) named g.LADYbird, g.LADYbirdGND (for GND), and g.GAMMAearclip (for reference, ear-clip type) for recording EEG signals. These were driven by the power supply unit named g.GAMMAbox (g.tec). Twenty five electrodes in accordance with the 10-5 system [19] were placed at CPz, CP1, CP2, CP3, CP4, CP5, CP6, Pz, P1, P2, P3, P4, P5, P6, P7, P8, POz, PO3, PO4, PO7, PO8, Oz, O1, O2 and Iz. The electrodes for GND and reference were positioned at AFz and A1, respectively.

2.2. SSVEP Recognition Using MCCA

The authors have recently proposed a novel method to recognize mixed-coded SSVEPs which achieved high performance [16]. The method employs multiset canonical correlation analysis (MCCA) [20] to obtain a spatial filter which enhances SSVEP components.

MCCA is a generalization of CCA to multiple datasets [20–24]. It finds weight vectors that maximize a correlation between weighted linear combinations of each dataset, called canonical variates. Let $\mathbf{S}_i \in \mathbb{R}^{I_i \times N}$ $(i = 1, \ldots, Q)$ be an I_i-channel signal that is normalized to have zero mean and unit variance. Their linear combinations, canonical variates, are denoted by $\mathbf{w}_i^T \mathbf{S}_i$, where $\mathbf{w}_i \in \mathbb{R}^{I_i \times 1}$ is a weight vector. With the MAXVAR criterion [20, 22, 23], MCCA solves the following maximization problem to find weight vectors $\mathbf{w} = [\mathbf{w}_1^T, \mathbf{w}_2^T, \cdots, \mathbf{w}_Q^T]^T$:

$$\rho = \max_{\mathbf{w}_1, \ldots, \mathbf{w}_Q} \sum_{i \neq j}^{Q} \mathbf{w}_i^T \mathbf{S}_i \mathbf{S}_j^T \mathbf{w}_j \quad \text{s.t.} \ \frac{1}{Q} \sum_{i=1}^{Q} \mathbf{w}_i^T \mathbf{S}_i \mathbf{S}_i^T \mathbf{w}_i = 1. \tag{1}$$

Using a Lagrange multiplier technique, this objective function can be transformed into a generalized eigenvalue problem. The eigenvectors corresponding to the eigenvalues sorted in a descending order and the largest eigenvalue are denoted by $\mathbf{w}_i^{(1)}, \mathbf{w}_i^{(2)}, \ldots, \mathbf{w}_i^{(\Sigma_i I_i)}$ and λ, respectively. The largest eigenvalue can be interpreted as the similarity of those multiple datasets and the eigenvectors corresponding to the large eigenvalues can be interpreted as the weight vectors that increase the correlation between these datasets.

In accordance with [16], MCCA was applied substituting the EEG signal of test data $\mathbf{x}$ for $\mathbf{S}_1$, the artificial reference signal $\mathbf{y}_k$ for $\mathbf{S}_2$, and the individual template $\mathbf{z}_k$ for $\mathbf{S}_3$, where the subscript, k, describes the index for stimuli. If the kth stimulus has a frequency of f_k, then the artificial signal $\mathbf{y}_k$ consisted of Fourier series of simulated stimulus signals given as

$$\mathbf{y}_k = [\sin(2\pi f_k t), \cos(2\pi f_k t), \ldots, \sin(2L\pi f_k t), \cos(2L\pi f_k t)]^T, \tag{2}$$

where L is the number of harmonics in the Fourier series, the first two components are the sinusoids of the fundamental frequency f_k and the others are harmonics. The number of harmonics was set to $L = 3$ in the present study. Additionally, the individual template $\mathbf{z}_k$ corresponding to the kth stimulus was obtained by averaging EEG signals in a calibration dataset across trials. Applying MCCA to these datasets, the largest eigenvalue λ_k and a spatial filter $\mathbf{w}_\mathbf{x}$ that was an eigenvector corresponding to the largest eigenvalue were obtained. With the spatial filter, the test signal $\mathbf{x}$ and the individual template $\mathbf{z}_k$ were projected. Subsequently, correlation coefficients between these two projections were obtained as:

$$\rho_k = \mathrm{Corr}\left(\mathbf{w}_\mathbf{x}{}^T \mathbf{x}, \mathbf{w}_\mathbf{x}{}^T \mathbf{z}_k\right), \tag{3}$$

where $\mathrm{Corr}(\cdot, \cdot)$ is the Pearson's correlation coefficient. The correlation coefficients were computed for each command k $(k = 1, \ldots, K)$ following Equation (3). The largest eigenvalue and the correlation coefficient were combined and used for detecting a command as follows:

$$k^\star = \underset{k}{\mathrm{argmax}} \ \lambda_k \mathrm{sign}\left(\rho_k\right) \cdot \left(\rho_k\right)^2. \tag{4}$$

2.3. Transferring the Source Template

As described earlier, the individual templates can be obtained by averaging EEG signals across trials for each command. Necessarily, it requires a long time for calibration. To overcome this issue,

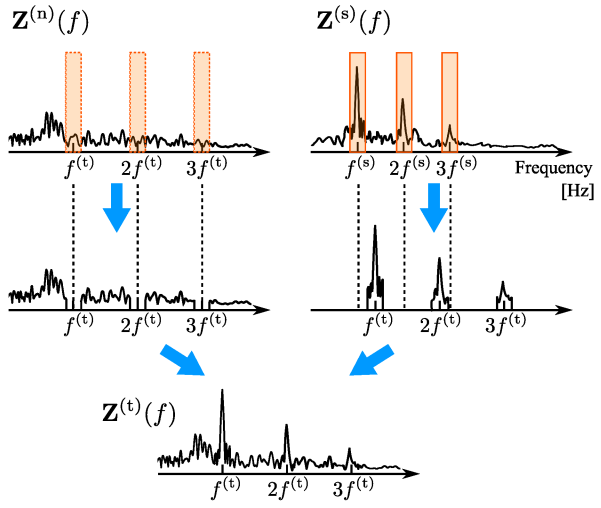

Fig. 2: Frequency shifting by a bank of bandpass filters and a bank of bandstop filters. Fourier transforms of the non-control EEG signal, the source template, and the target template are denoted by $\mathbf{Z}^{(\mathrm{n})}(f)$, $\mathbf{Z}^{(\mathrm{s})}(f)$, and $\mathbf{Z}^{(\mathrm{t})}(f)$, respectively.

we aimed to transfer the individual template of a certain command, named a source template, to obtain a new template of the other command, named a target template. The source template can be transferred to the target template by these two following approaches:

Shifting the phase A source template is shifted in time domain with a time delay which corresponds to a phase desired to be shifted;

Shifting the frequency A source template is Fourier transformed into a frequency domain. Subsequently, the peak at a source frequency is shifted to a target frequency and inverse transformed into a time domain.

Details for these approaches are described below.

2.3.1. *Shifting the phase*

Let $\mathbf{z}^{(\mathrm{s})}(t)$ be a source template given as an average of the recorded EEG signals as a response to a visual stimulus flickering with a certain frequency $f^{(\mathrm{s})}$ and a phase $\phi^{(\mathrm{s})}$. A target template $\mathbf{z}^{(\mathrm{t})}(t)$ with the same frequency $f^{(\mathrm{s})}$ as the source template and a target phase $\phi^{(\mathrm{t})}$ is obtained by shifting the source template with a time delay as follows:

$$\mathbf{z}^{(\mathrm{t})}(t) = \mathbf{z}^{(\mathrm{s})}(t+\tau), \tag{5}$$

where the time delay τ is defined as $\tau = \frac{\phi^{(\mathrm{t})}-\phi^{(\mathrm{s})}}{2\pi f^{(\mathrm{s})}}$.

2.3.2. *Shifting the frequency*

The following procedure is based on an assumption that base lines of Fourier transforms of the source template and the target template share a common characteristic, and that common characteristic would appear in EEG signals in non-control state. The EEG signals in non-control state, i.e., when the user is not gazing at any visual stimulus, would represent a background activity, a spontaneous activity, an environmental noise, and so forth. Accordingly, the target template in frequency domain can be ideally obtained by exploiting non-control EEG signals as a base line and shifting the peaks of the source template at a source frequency to a target frequency. Fig. 2 illustrates an image of the proposed architecture of frequency shifting.

Let $\mathbf{Z}^{(\mathrm{s})}(f)$ and $\mathbf{Z}^{(\mathrm{n})}(f)$ be Fourier transforms of the source template and the non-control EEG signal, respectively. Firstly, Fourier transform of the source template $\mathbf{Z}^{(\mathrm{s})}(f)$ was filtered by a bank of bandpass filters that passes the harmonics corresponding to the source frequency, $f^{(\mathrm{s})}$, of the source template. Specifically, the outputs of the filter bank are denoted by

$$\mathbf{Z}_1^{(\mathrm{s})}(f) = \mathcal{H}_{f^{(\mathrm{s})}}(f)\mathbf{Z}^{(\mathrm{s})}(f), \tag{6}$$

$$\vdots$$

$$\mathbf{Z}_L^{(\mathrm{s})}(f) = \mathcal{H}_{Lf^{(\mathrm{s})}}(f)\mathbf{Z}^{(\mathrm{s})}(f), \tag{7}$$

where L is the number of harmonics and $\mathcal{H}_{\overline{f}}(f)$ is the transfer function of a bandpass filter at the center frequency of $\overline{f}$ with a bandwidth of $2\Delta f$, defined as:

$$\mathcal{H}_{\overline{f}}(f) = \begin{cases} 1, & \overline{f}-\Delta f \le f \le \overline{f}+\Delta f \\ 0, & \text{otherwise} \end{cases}, \tag{8}$$

where Δf was set to 0.5 Hz in the present study. Secondly, Fourier transform of the non-control signal $\mathbf{Z}^{(\mathrm{n})}(f)$ was filtered by a bank of bandstop filters so as to exclude bands corresponding to the target frequency $f^{(\mathrm{t})}$ and its harmonics, and then, previously extracted peaks corresponding to the source frequency was shifted to a target frequency and added as follows:

$$\begin{aligned}\mathbf{Z}^{(\mathrm{t})}(f) = &\left\{\overline{\mathcal{H}}_{f^{(\mathrm{t})}}(f) + \overline{\mathcal{H}}_{2f^{(\mathrm{t})}}(f) + \cdots + \overline{\mathcal{H}}_{Lf^{(\mathrm{t})}}(f)\right\}\mathbf{Z}^{(\mathrm{n})}(f) \\ &+ \mathbf{Z}_1^{(\mathrm{s})}\left(f - \left(f^{(\mathrm{t})} - f^{(\mathrm{s})}\right)\right) \\ &+ \mathbf{Z}_2^{(\mathrm{s})}\left(f - \left(2f^{(\mathrm{t})} - 2f^{(\mathrm{s})}\right)\right) \\ &+ \cdots + \mathbf{Z}_L^{(\mathrm{s})}\left(f - \left(Lf^{(\mathrm{t})} - Lf^{(\mathrm{s})}\right)\right),\end{aligned} \tag{9}$$

where $\overline{\mathcal{H}}_{\overline{f}}(f)$ is the transfer function of a bandstop filter at the center frequency of $\overline{f}$ with a bandwidth of $2\Delta f$, defined as:

$$\overline{\mathcal{H}}_{\overline{f}}(f) = \begin{cases} 0, & \overline{f}-\Delta f \le f \le \overline{f}+\Delta f \\ 1, & \text{otherwise} \end{cases}. \tag{10}$$

Finally, the target template $\mathbf{z}^{(\mathrm{t})}(t)$ with the target frequency $f^{(\mathrm{t})}$ and the same phase $\phi^{(\mathrm{s})}$ as the source template was obtained by the inverse Fourier transform of $\mathbf{Z}^{(\mathrm{t})}(f)$.

2.3.3. *Case study for transferring the source template*

Consider a set of mixed-coded stimuli consisting of $N_f \times N_p$ commands in total, where N_f and N_p are the number of different frequencies and phases that are assigned to each visual stimulus. This paper assumed the following three cases:

Phase-shifted template (PST) As source templates, use EEG signals with respect to visual stimuli of N_f different frequencies. PST is obtained by shifting the phase of each source template.

Frequency-shifted template (FST) As source templates, use EEG signals with respect to visual stimuli of N_p different phases and one phase. PST is obtained by shifting the frequency of each source template.

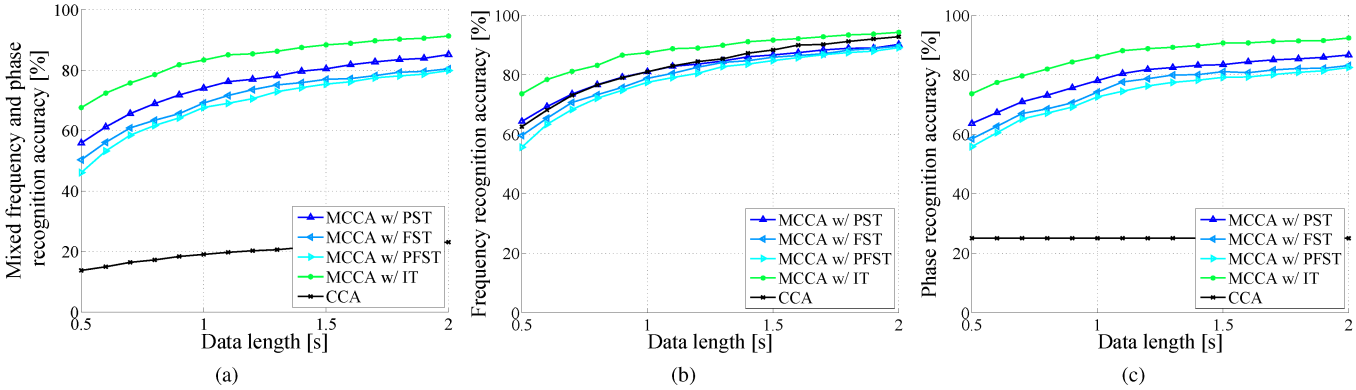

Fig. 3: Averaged recognition accuracies across the subjects of (a) mixed frequency and phase, (b) frequency, and (c) phase. Blue lines with triangle markers shows the results based on the proposed approach, and the other two lines shows the results based on the prior works.

Table 1: Averaged mixed frequency and phase recognition accuracy (MACC), frequency recognition accuracy (FACC), phase recognition accuracy (PACC) across the subjects using the data length of 2.0 seconds. The top three rows show the results based on the proposed approach, and the lower two row shows that based on the prior works.

Method	MACC [%]	FACC [%]	PACC [%]
MCCA w/ PST	85.17 ± 15.04	90.23 ± 11.39	86.68 ± 13.33
MCCA w/ FST	80.45 ± 16.72	89.69 ± 11.04	83.13 ± 13.98
MCCA w/ PFST	79.86 ± 18.38	89.12 ± 14.21	82.47 ± 15.00
MCCA w/ IT	91.31 ± 11.67	94.32 ± 8.97	92.39 ± 10.02
CCA	23.04 ± 2.25	92.81 ± 9.62	25.00 ± 0.00

Phase-and-frequency-shifted template (PFST) As a source template, use EEG signals with respect to a visual stimulus of one phase and one phase. PFST is obtained by shifting both the phase and frequency of the source template.

In this paper, the individual templates with the frequency $f^{(s)} = 15$ Hz and $\phi^{(s)} = 180$ degrees were employed as the source templates to obtain the PSTs and FSTs, respectively. For the PFSTs, the individual template with the frequency $f^{(s)} = 15$ Hz and $\phi^{(s)} = 180$ degrees was employed as the source template. The non-control signal was obtained by averaging EEG signals of pre-flickering interval. Furthermore, the phase was first shifted and the frequency was shifted next to obtain the PFSTs.

3. RESULTS

To evaluate performance, mixed frequency and phase, frequency, and phase recognition accuracy were measured, respectively. These accuracies using MCCA with PST, FST, and PFST were compared with the previous works including MCCA with individual template (IT) [16] and the standard CCA method [25, 26] for the reference methods. It should be noted that MCCA with IT need a full calibration, while the standard CCA cannot decode a phase. The performance of these methods were evaluated based on 4-fold cross-validation.

Figs. 3a, 3b, and 3c show the averaged recognition accuracies of mixed frequency and phase, frequency only, and phase only. Table 1 summarizes the averaged accuracies across the subjects using the data length of 2.0 seconds. As shown in Figs. 3a, 3b, and 3c, MCCA with IT achieved the highest accuracy compared to the other methods in either case of recognizing the mixed frequency and phase, the frequency, and the phase as expected. Among the proposed approaches, PST achieved a slightly higher accuracy compared to FST. Remarkably, PFST which required only one source template also performed well closely achieving to FST and PST as shown in Table 1. Besides, in terms of the frequency recognition, MCCA with PST, FST, and PFST was inferior to the standard CCA as presented in Fig. 3b. However, it is worth noting that MCCA with PST, FST, and PFST can be applied to the phase recognition and the mixed frequency and phase recognition as well.

4. DISCUSSIONS

The experimental results showed that the proposed transferred template enabled to recognize both frequency and phase with a small amount of calibration closely achieving the performance using the full calibration data. The difference between the highest accuracies using the transferred templates and the individual templates was −11.45%, while the minimum time for calibration could be decreased by 93.75%.

Although mixed-coded SSVEP-BCI was employed to evaluate the proposed transferring approach in this paper, PFST can be applied to joint-coded SSVEP-BCIs likewise. This means that this study is potentially applicable to many of existing calibration-based algorithms [11, 15, 27] for recognition of the frequency and phase of SSVEPs. In the case of applying PFST, the minimum time for calibration would be reduced by $1/$*the number of commands in total*, which is an important improvement for a practical use.

As described in Section 3, the frequency recognition accuracy using the proposed approach was slightly lower than that of the standard CCA method [25]. Hence, further studies might explore how to shift the frequency in a more sophisticated manner in order to achieve higher performance. Moreover, an online adaptation of the transferred templates [17] would also improve the performance and help us to establish a more reliable interface.

In conclusion, this paper proposed an innovative approach to calibration reduction for hybrid frequency and phase coded SSVEP-BCIs. The present results suggested the feasibility of the proposed approach to achieve a high performance with a small calibration.

5. REFERENCES

[1] Jean-Jacques Vidal, "Toward direct brain–computer communication," *Annu. Review of Biophysics and Bioeng.*, vol. 2, no. 1, pp. 157–180, 1973.

[2] Jonathan R Wolpaw, Niels Birbaumer, Dennis J McFarland, Gert Pfurtscheller, and Theresa M Vaughan, "Brain–computer interfaces for communication and control," *Clinical Neurophysiology*, vol. 113, no. 6, pp. 767–791, June 2002.

[3] Lawrence Ashley Farwell and Emanuel Donchin, "Talking off the top of your head: Toward a mental prosthesis utilizing event-related brain potentials," *Electroencephalography and Clinical Neurophysiology*, vol. 70, no. 6, pp. 510–523, Dec. 1988.

[4] Jonathan R Wolpaw, Dennis J McFarland, Gregory W Neat, and Catherine A Forneris, "An EEG-based brain–computer interface for cursor control," *Electroencephalography and clinical neurophysiology*, vol. 78, no. 3, pp. 252–259, 1991.

[5] Ming Cheng, Xiaorong Gao, Shangkai Gao, and Dingfeng Xu, "Design and implementation of a brain–computer interface with high transfer rates," *IEEE Transactions on Biomedical Engineering*, vol. 49, no. 10, pp. 1181–1186, 2002.

[6] Matthew Middendorf, Grant McMillan, Gloria Calhoun, Keith S Jones, et al., "Brain–computer interfaces based on the steady-state visual-evoked response," *IEEE Trans. Neural Syst. Rehab. Eng.*, vol. 8, no. 2, pp. 211–214, 2000.

[7] Hovagim Bakardjian, Toshihisa Tanaka, and Andrzej Cichocki, "Optimization of SSVEP brain responses with application to eight-command brain–computer interface," *Neuroscience Letters*, vol. 469, no. 1, pp. 34–38, 2010.

[8] Y. Kimura, T. Tanaka, H. Higashi, and N. Morikawa, "SSVEP-based brain–computer interfaces using FSK-modulated visual stimuli," *IEEE Trans. Biomed. Eng.*, vol. 60, no. 10, pp. 2831–2838, Oct. 2013.

[9] Hiroshi Higashi and Toshihisa Tanaka, "Common spatio-time-frequency patterns for motor imagery-based brain machine interfaces," *Computational Intelligence and Neuroscience*, vol. 2013, pp. 8, 2013.

[10] Kaori Suefusa and Toshihisa Tanaka, "Phase-based detection of intentional state for asynchronous brain–computer interface," in *2015 IEEE International Conference on Acoustics, Speech and Signal Processing (ICASSP)*. IEEE, 2015, pp. 808–812.

[11] Xiaogang Chen, Yijun Wang, Masaki Nakanishi, Xiaorong Gao, Tzyy-Ping Jung, and Shangkai Gao, "High-speed spelling with a noninvasive brain–computer interface," *Proceedings of the National Academy of Sciences*, vol. 112, no. 44, pp. E6058–E6067, 2015.

[12] Xiaogang Chen, Yijun Wang, Masaki Nakanishi, Tzyy-Ping Jung, and Xiaorong Gao, "Hybrid frequency and phase coding for a high-speed SSVEP-based BCI speller," in *2014 36th Annual International Conference of the IEEE Engineering in Medicine and Biology Society*. IEEE, 2014, pp. 3993–3996.

[13] Chuan Jia, Xiaorong Gao, Bo Hong, and Shangkai Gao, "Frequency and phase mixed coding in SSVEP-based brain–computer interface," *IEEE Transactions on Biomedical Engineering*, vol. 58, no. 1, pp. 200–206, 2011.

[14] Yu-Te Wang, Masaki Nakanishi, Simon Lind Kappel, Preben Kidmose, Danilo P Mandic, Yijun Wang, Chung-Kuan Cheng, and Tzyy-Ping Jung, "Developing an online steady-state visual evoked potential-based brain-computer interface system using EarEEG," in *2015 37th Annual International Conference of the IEEE Engineering in Medicine and Biology Society (EMBC)*. IEEE, 2015, pp. 2271–2274.

[15] Masaki Nakanishi, Yijun Wang, Yu-Te Wang, Yasue Mitsukura, and Tzyy-Ping Jung, "A high-speed brain speller using steady-state visual evoked potentials," *International Journal of Neural Systems*, vol. 24, no. 06, pp. 1450019, 2014.

[16] Kaori Suefusa and Toshihisa Tanaka, "Decoding of responses to mixed frequency and phase coded visual stimuli using multiset canonical correlation analysis," in *2016 38th Annual International Conference of the IEEE Engineering in Medicine and Biology Society*. IEEE, 2016, pp. 1492–1495.

[17] Peng Yuan, Xiaogang Chen, Yijun Wang, Xiaorong Gao, and Shangkai Gao, "Enhancing performances of SSVEP-based brain–computer interfaces via exploiting inter-subject information," *Journal of Neural Engineering*, vol. 12, no. 4, pp. 046006, 2015.

[18] Yijun Wang, Y-T Wang, and T-P Jung, "Visual stimulus design for high-rate SSVEP BCI," *Electronics letters*, vol. 46, no. 15, pp. 1057–1058, 2010.

[19] Robert Oostenveld and Peter Praamstra, "The five percent electrode system for high-resolution EEG and ERP measurements," *Clinical Neurophysiology*, vol. 112, no. 4, pp. 713–719, 2001.

[20] Jon R Kettenring, "Canonical analysis of several sets of variables," *Biometrika*, vol. 58, no. 3, pp. 433–451, 1971.

[21] Javier Vía, Ignacio Santamaría, and Jesús Pérez, "A learning algorithm for adaptive canonical correlation analysis of several data sets," *Neural Networks*, vol. 20, no. 1, pp. 139–152, 2007.

[22] Allan Aasbjerg Nielsen, "Multiset canonical correlations analysis and multispectral, truly multitemporal remote sensing data," *IEEE Transactions on Image Processing*, vol. 11, no. 3, pp. 293–305, 2002.

[23] Yu Zhang, Guoxu Zhou, Jing Jin, Xingyu Wang, and Andrzej Cichocki, "Frequency recognition in SSVEP-based bci using multiset canonical correlation analysis," *International Journal of Neural Systems*, vol. 24, no. 04, pp. 1450013, 2014.

[24] Yi-Ou Li, Tülay Adali, Wei Wang, and Vince D Calhoun, "Joint blind source separation by multiset canonical correlation analysis," *IEEE Transactions on Signal Processing*, vol. 57, no. 10, pp. 3918–3929, 2009.

[25] Zhonglin Lin, Changshui Zhang, Wei Wu, and Xiaorong Gao, "Frequency recognition based on canonical correlation analysis for SSVEP-based BCIs," *IEEE Trans. Biomed. Eng.*, vol. 53, no. 12, pp. 2610–2614, Dec. 2006.

[26] Harold Hotelling, "Relations between two sets of variates," *Biometrika*, vol. 28, no. 3, pp. 321–377, Dec. 1936.

[27] Masaki Nakanishi, Yijun Wang, Yu-Te Wang, and Tzyy-Ping Jung, "A dynamic stopping method for improving performance of steady-state visual evoked potential based brain-computer interfaces," in *2015 37th Annual International Conference of the IEEE Engineering in Medicine and Biology Society (EMBC)*. IEEE, 2015, pp. 1057–1060.